ELSEVIER

Atomic-level molecular modeling of the nonionic surfactant Triton X-100: The OPE_9 component in vacuum and water

Agnes Derecskei-Kovacs,* Bela Derecskei,* and Zoltan A. Schelly†

**Department of Chemistry, Texas A&M University, College Station, Texas USA*
†Center for Colloidal and Interfacial Dynamics, University of Texas at Arlington, Arlington, Texas USA

The commercially available nonionic surfactant Triton X-100 is a mixture of polyoxyethylene tert-octylphenyl ethers (OPE_n) with an average of n = *9.5 oxyethylene (OE) units in the molecules, and the population maximum at* n = *9. Thus, the $OPE_{n=9}$ component was chosen to be studied by atomic level molecular modeling, using second-generation force fields. The 1,000 conformers generated via random sampling of torsional angles around single bonds yielded 11 clusters based on geometrical similarity. Representatives of geometrically distinctly different clusters with significant populations were chosen from a narrow energy range around the most probable energy to be analyzed for interaction with water. The effect of water on the conformation of the OE chain was found to be modest, similar to the situation that had been reported earlier for the anionic surfactant Aerosol-OT (AOT). The number of bound water molecules is strongly dependent on the conformation of the OE chain and is affected by electrostatic as well as steric effects. Unlike the case of AOT, for which the length of the hydrophobic tail was found to govern the size of reverse micelles in CCl_4, the size of reverse micelles of $OPE_{n=9}$ cannot be predicted from the dimensions of the hydrophilic tail. © 1999 by Elsevier Science Inc.*

Keywords: solvent interaction, molecular mechanics, atomic simulation, surfactant modeling, polyoxyethylene tert-*octylphenyl ether, reverse micelle*

INTRODUCTION

The commercially available surfactant Triton X-100 is one of the most commonly used nonionic surfactants[1,2] in technical and scientific applications. It consists of a mixture of polyoxyethylene *tert*-octylphenyl ethers (OPE_n; Figure 1) with an average of $n = 9.5$ oxyethylene (OE) units in the molecules and the population maximum at $n = 9$[3] and belongs to the widely used family of polyoxyethylene-base surfactants.[4–6]

Triton X-100 as well as the pure $OPE_{n=9}$ component form a variety of organized assemblies (micelle, reverse micelle, liquid crystal, gel, etc.) in solution depending on the nature of the solvent, the concentration of the surfactant, temperature, etc.[7] In cyclohexane, OPE_n components with similar chain lengths ($\Delta n \sim 1$–2) exhibit similar phase behavior.[3] With increasing length of the hydrophilic chain, the solubility of the surfactant in nonpolar solvents decreases. In ternary reverse micellar systems, the amount of water that can be solubilized in the polar core of the aggregates, of course, increases with the length of the OE chain. Hence, as the component that has the highest population in the mixture, OPE_9 is investigated in the present study for a characterization of Triton X-100.

Computer simulation of the amphiphilic behavior of surfactants may be performed at least at two different levels of complexity. The dynamics of the self-aggregation process on a relatively large time scale may be investigated by using a simple model consisting of "water-like" particles, "oillike" particles, and "surfactant-like" molecules constructed of the former two moieties.[8–10] Conversely, in the atomic approximation, molecules are modeled more realistically by invoking the usual stretching, bending, torsion and nonbonded interactions. Although more detailed qualitative and quantitative information may be obtained about the system at this level, the affordable time scale of the simulations is too short for examining some of the important dynamic processes involved in self-aggregation. Nevertheless, atomic description of amphiphilic systems has been successfully implemented for a number of micelles.[11–19] In the present study, atomic level modeling of OPE_9 is used for assessing the behavior of one representative molecule in vacuum and its interaction with water.

The aim of such investigations is to obtain insight about the geometry (i.e., the probable conformations) of the surfactant

Color Plates for this article are on pages 258–260.

Address reprint requests to: Dr. Agnes Derecskei-Kovacs, Department of Chemistry, Texas A&M University, College Station, TX 77842-3012 USA.

Journal of Molecular Graphics and Modelling 16, 206–212, 1998

655 Avenue of the Americas, New York, NY 10010

1093-3263/99/$–see front matter
PII S1093-3263(99)00011-X

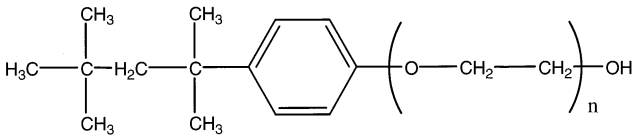

Figure 1. Formula of Triton X-100. In the commercially available surfactant, $n = 9.5$.

and quantitative data on the number and binding sites of bound water molecules. This information is useful for designing compartmentalized systems such as reverse micelles and water-in-oil microemulsions that are often utilized for the encapsulation of hydrophilic substrates. In such applications, the size and nature of the aqueous pools in the interior of the aggregates greatly determine the extent of solubilization and the reactivity of the substrate. These, however, can be tailored by the proper choice of oxyethylene chain lengths and the relative amounts in which different chain lengths are present.

In the formation of organized assemblies, the packing of amphiphiles in the aggregates is mainly governed by the overall geometry of the surfactant molecule and the extent of hydration of its hydrophilic moiety (OE chain in the present case). Thus, our atomic level molecular modeling of OPE_9 using second-generation force fields is focused on finding a conformer distribution via random sampling and the investigation of the interaction of representative conformers with water.

METHODS

Conformer search

The starting geometry for the conformer search of OPE_9 was generated by geometry optimization of the molecule constructed from simple organic fragments (Figure 1). Rotations around each single bond were allowed with the exception of single bonds involving terminal hydrogen atoms. One thousand initial conformations were generated by random sampling of the full range of the remaining 30 torsional angles. The structures were then fully optimized.

All conformer search calculations were carried out on an SGI O2 workstation, using the second-generation Universal Force Field[20] (UFF) as it is currently implemented in the commercially available Cerius[2] program package (version 3.5) developed by Molecular Simulations, Inc.[21] UFF is a rule-based force field that yields accurate molecular geometries and conformational energy differences for a wide range of atoms in very different chemical environments.[22–24]

Clustering

The resultant optimal geometries are classified by using the "autocluster" utility in Cerius[2]. During this procedure, all conformers are sorted by energy. The lowest-energy conformation is chosen as the nucleus of the first cluster. The rms difference

$$\sum_{i \in \text{all atoms}} [(x_i - x_r)^2 + (y_i - y_r)^2 + (z_i - z_r)^2]^{1/2}$$

of all the other conformations with respect to this cluster nucleus is calculated. All conformations that have an rms difference below the threshold are assigned to this first cluster. The threshold value is preselected by calculating all the pairwise rms differences (difference index) and plotting the number of conformer pairs as a function of the rms difference. The threshold value is selected at the maximum of this curve as the most probable difference index (4.55 in our case) of the conformer ensemble. As the next step of the clustering procedure, the lowest energy conformation of the remaining set of unclustered conformations is chosen as the nucleus of the second cluster and the rms difference of all the other conformers with respect to this reference is calculated. The procedure is repeated until all conformers are assigned to a cluster.

Interaction with water

In order to investigate the interaction between the OPE_9 molecule and a hydrate layer consisting of a large number of water molecules, one conformer was chosen from each geometry cluster having a statistically significant population. The majority of conformers of the total ensemble were found to be in a narrow energy range. Therefore, one representative conformer was chosen randomly from each cluster from a 2 kcal/mol energy window around the most probable energy of the total ensemble. Then, the representative conformers were reoptimized by using the Extensible Systematic Force Field (ESFF) in Insight 97 as implemented by Molecular Simulations, Inc.[21] (The switch of force fields was necessary since the atomic level treatment of solvent interactions is readily available in Insight 97 through solvent boxes. Solvent boxes model bulk solvents through an equilibrated ensemble of solvent molecules adjusted to simulate the macroscopic density at a given temperature. However, Insight 97 does not link up with the Universal Force Field; therefore, ESFF was used from the same class of force fields for further studies. Cerius[2], although does not offer solvent boxes, it is readily applicable for the type of conformer search and analysis chosen for this study.) The resultant struc-

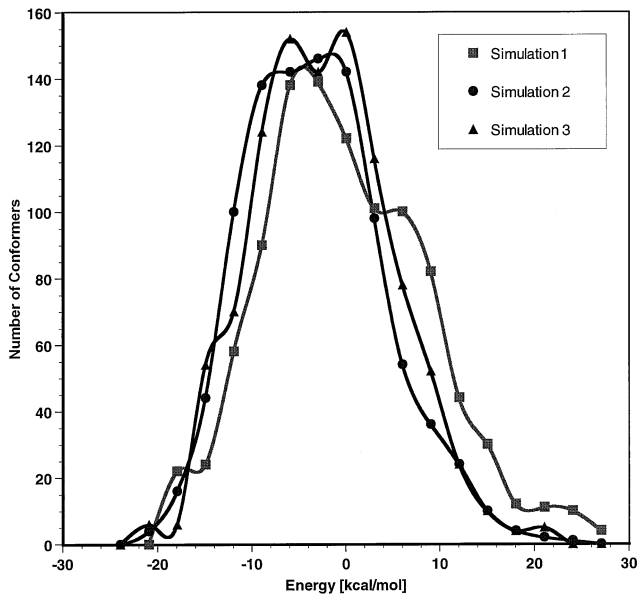

Figure 2. Energy distributions of the unique conformers of the OPE_9 molecule generated by three random sampling simulations. All conformers were minimized by the UFF force field.

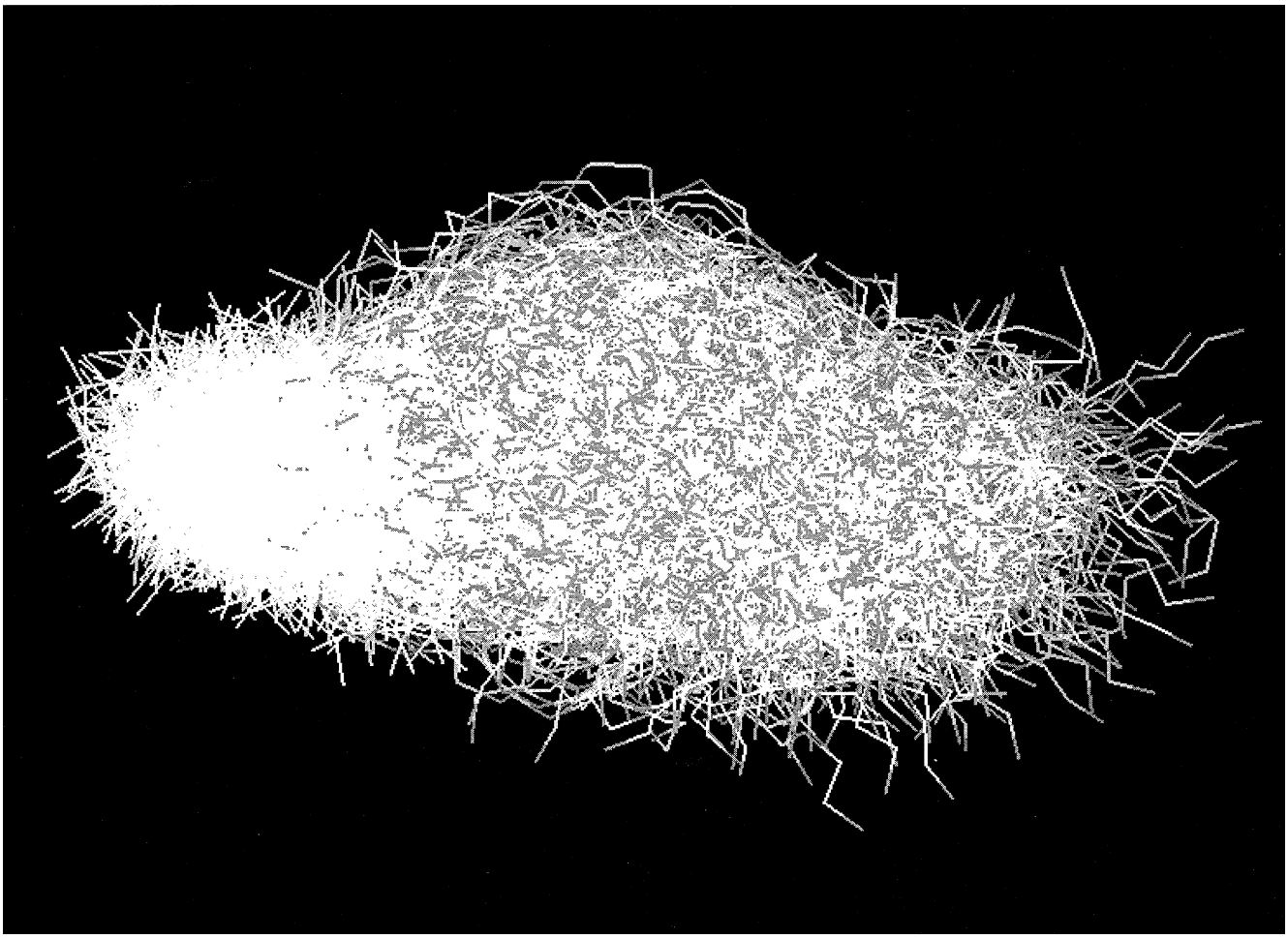

Figure 3. Overlay of 998 unique, geometry-optimized conformers generated via random sampling of 30 torsional angles in the OPE_9 molecule as calculated with the UFF force field.

tures of optimal energy were "soaked" by surrounding them with a 5-Å-thick water layer (earlier,[25] this thickness was found to be a satisfactory compromise between accuracy and computational speed). The hydrated systems were optimized using the ESFF force field, and the results were analyzed with respect to the effects of solvation.

RESULTS AND DISCUSSION

Conformer search

The majority of single bonds are located in the polyoxyethylene region of OPE_9 (Color Plate 1). Considering all of the degrees of torsional freedom (tail and head) leads to an astronomical number of possible conformers. Our goal was not a systematic and complete mapping of the conformer space but a finite sampling that would reveal a possible correlation between geometry and energy. For this purpose, we generated 1 000 conformers by random sampling of the full range of the 30 angles that were allowed to vary. The procedure yielded 998 unique structures. From this ensemble, we chose two conformations as the starting geometries for two additional independent conformer searches. (The reasoning behind the choice of conformers is described in the section Clustering and Analysis of the Clusters.) The distributions of the relative energy obtained in the three searches are shown in Figure 2.

As can be seen from Figure 2, a large number of conformers are found in a relatively narrow energy range (approximately 15 kcal/mol wide) around the population maximum. The distributions are approximately 50 kcal/mol wide with only a few conformers with significantly higher energies. There were a few conformers (less than 0.2%) which were not fully optimized during the search procedure, and were omitted from further consideration. The three independent conformer searches yielded energy distributions of similar width and height in spite of the significantly different starting geometries used. Figure 3 shows the overlay of the 998 conformers generated in the first conformer search.

The image reflects the flexibility of the OPE_9 molecule. The head and tail portions of the molecule are clearly distinguishable but all the finer details are hidden behind a large number of different conformations derived from the almost free rotation around a large number of single bonds.

Clustering and analysis of the clusters

As mentioned earlier, the clustering procedure yielded 11 geometry classes (at a threshold index of 4.55) for the first

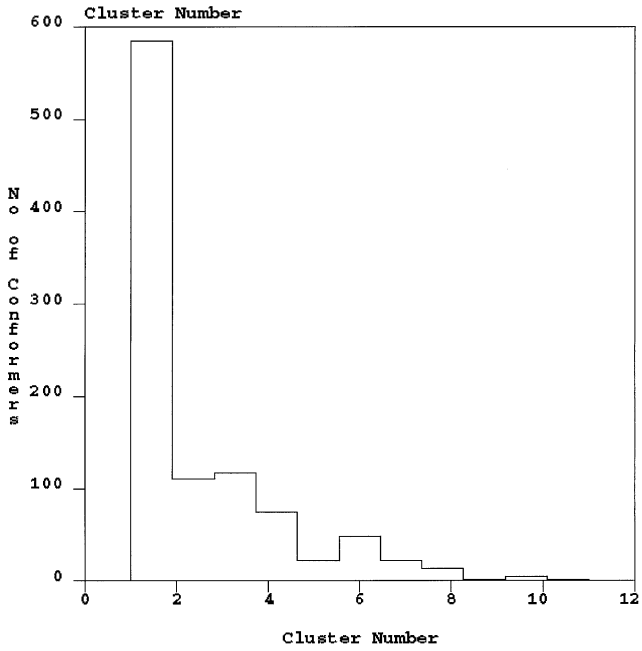

Figure 4. Population distribution over the 11 clusters of the 998 conformers depicted in Figure 3.

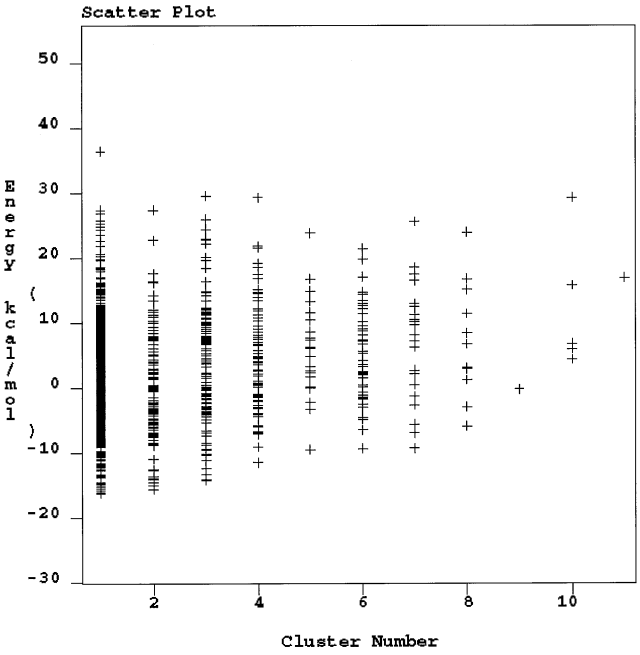

Figure 6. Scatter plot of relative energy versus cluster number for the 998 geometry-optimized conformers generated by random sampling of 30 torsional angles in OPE_9.

ensemble. The distribution of the 998 conformers over the clusters is shown on Figure 4.

It is clear from the figure that only 5 clusters (1, 2, 3, 4, and 6) have significant (>3%) populations. Three clusters (5, 7, and 8) have populations between 1 and 3%, and another three clusters (9, 10, and 11) have populations less than 1%. One representative each of clusters 1 and 6 was used as initial structures for the second and third independent follow-up con-

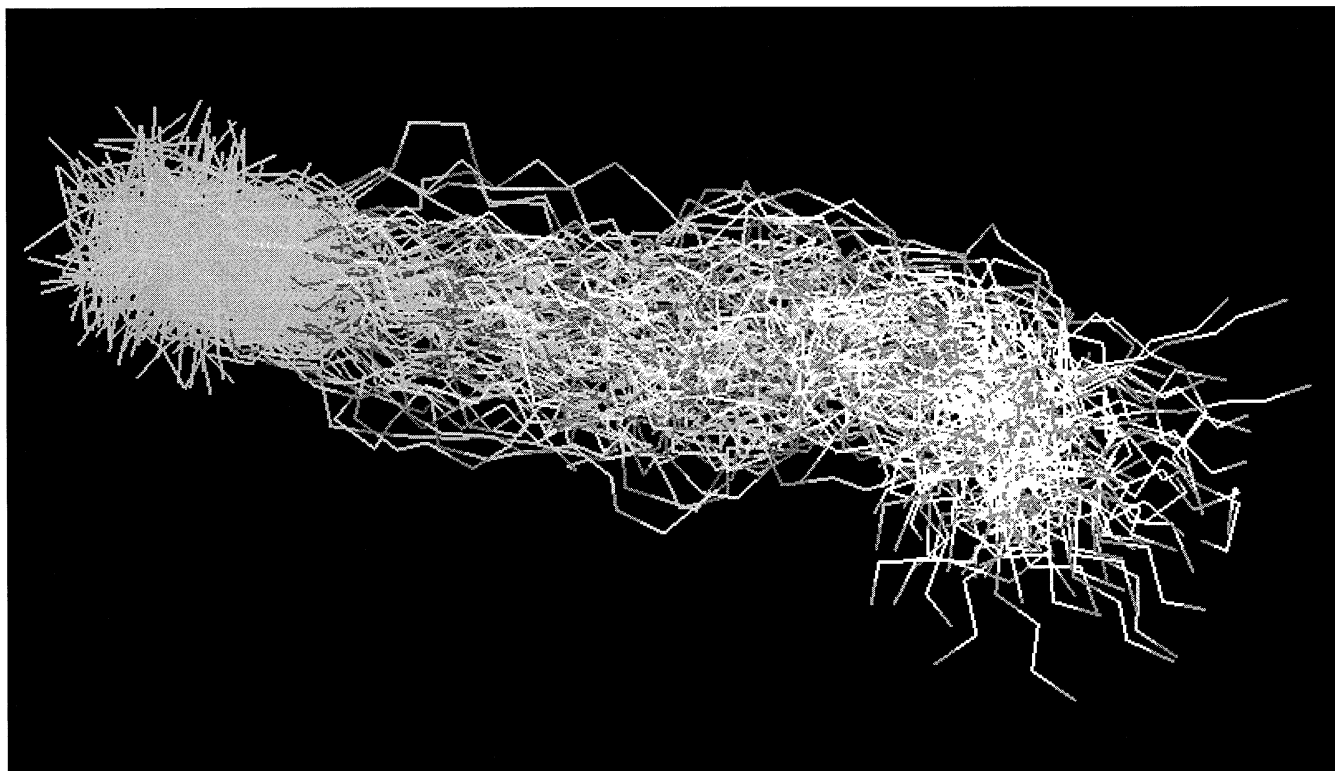

Figure 5. Overlay of 110 geometry optimized conformers in cluster 2 generated via random sampling of 30 torsional angles in OPE_9.

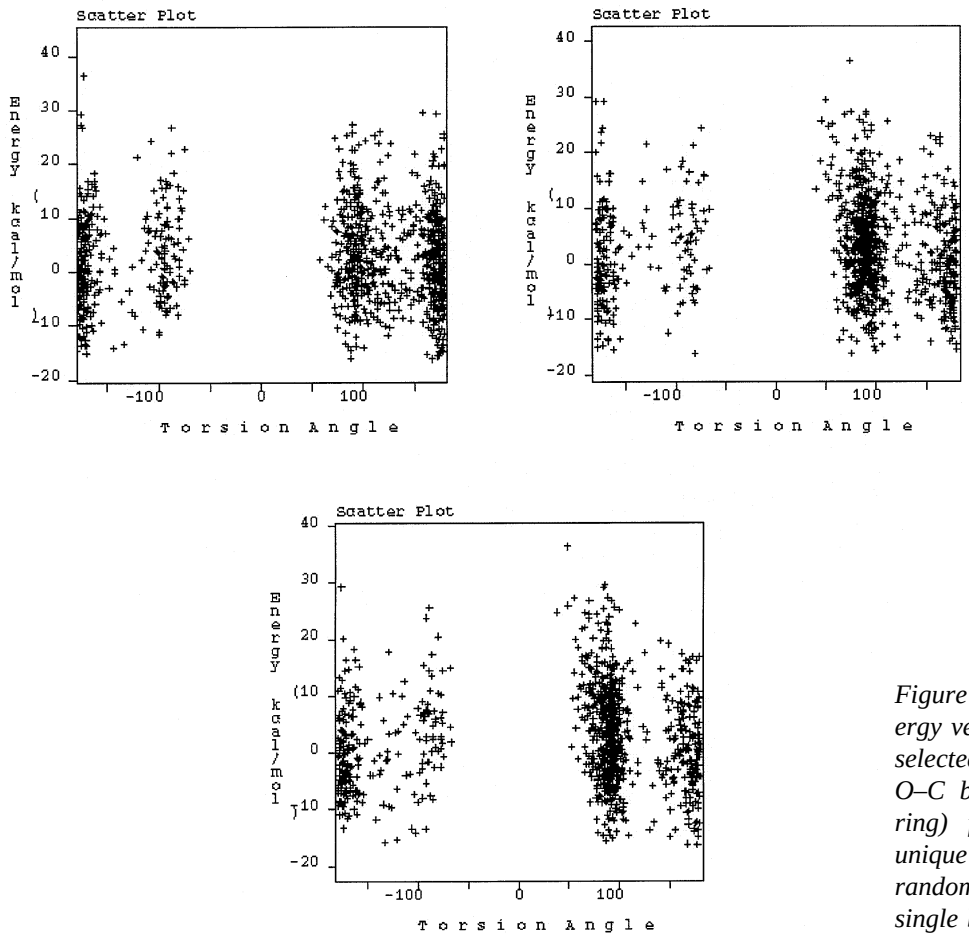

Figure 7. Individual scatter plots of energy versus torsional angle around three selected bonds (the third, fourth, and fifth O–C bonds, counted from the benzene ring) for the 998 geometry-optimized unique conformers of OPE_9 generated by random sampling of 30 torsions around single bonds.

former searches. These families have characteristically different shapes (cluster 1 is fairly linear and cluster 6 is very globular) in order to sample different areas on the conformer space. Since the geometrical clustering is performed in the order of increasing energy, the choice of representatives from these two clusters also entails the use of lower as well as higher energy starting geometries in the independent follow-up conformer searches. As an illustration of a family of geometries obtained in the first search, Figure 5 depicts an overlay of the 110 conformers in cluster 2. There is a long overall linear section close to the head and a pronounced C-shaped bending close to the end of the tail (see also Color Plate 1), characteristic of this particular family.

The clustering procedure was also performed for the second and third ensemble of conformers obtained through the independent searches. In spite of the very different initial geometries (and energies) used and the random nature of the search, the threshold indices were very similar (4.55, 4.38, 4.58). Also, the clustering consistently resulted in 5–6 clusters with statistically significant population, although the number of conformers in the individual clusters varied somewhat from ensemble to ensemble. The geometrical characteristics of these families (i.e., linear, C-shaped, S-shaped, globular, etc.) remained consistent throughout: The same geometry cluster families resulted from all three independent conformer searches, in spite of the different initial geometries and energies. Hence, it is reasonable to expect that although not all the possible conformers were derived, a representative model of the whole conformer space is obtained through the sampling.

Table 1. Energies (kcal/mol) of the five representative conformers of OPE_9 calculated with the UFF and ESFF force fields

	Conformer				
Force field	1	2	3	4	5
UFF	1.71	1.62	1.53	0.84	0.57
ESFF	31.92	31.03	27.22	26.87	24.39

Figure 6 shows a scatter diagram depicting the correlation (or the lack of it) between the energy and the geometry of the conformers. The diagram reveals no significant correlation between the energy and cluster number. Consequently, the torsional angle in a minimum energy conformation is not the defining factor for the energy, i.e., the molecule is rather insensitive to change in torsional angles. (Note, however, that we can compare energy differences between minima only, and no conclusion can be drawn about the height of the rotational barriers). A similar conclusion can be arrived at by analyzing the correlation diagrams between individual torsional angles and energy. An illustration is given in Figure 7. These scatter plots also reveal another characteristic feature of the confor-

Table 2. The number of hydrogen bonds at the beginning (n_i) and at the end (n_f) of geometry optimization, and the number of water molecules in the full soaking layer (N_{tot}) for the five representative conformers of the OPE_9 molecule as calculated with the ESFF force field

Conformer	n_i	n_f[a]	N_{tot}
1	2	12	198
2	3	9	170
3	0	10	148
4	1	11	144
5	0	5	124

[a] In contrast to the situation found for the anionic surfactant AOT,[25] none of the water molecules form more than one hydrogen bond with OPE_9. Separate simulations on $HO–CH_2–CH_2–OH$, in which a water molecule was initially forced to form hydrogen bonds with both oxygens of the glycol, resulted in breaking of at least one of the hydrogen bonds during minimization. Probably an *ab initio* study at least at the MP2 level could clarify the underlying reasons beyond the simple qualitative statement that one strong hydrogen bond seems to be energetically more favorable than two weak ones. In the case of the OPE_9 system, another possibility is that a second hydrogen bond is preferentially formed with another water molecule that is outside the primary solvent layer.

mations of OPE_9: For a given bond, only 2 or 3 distinct torsional angles occur with high probabilities, even though the total energy of the molecule may vary over a wide range. Similar observations were made earlier for the AOT molecule.[25]

Since details of the geometry do not seem to exert a large influence on the energy, one representative (having the most probable energy) from each of the five most populated clusters was randomly selected for further investigation (Color Plate 2).

Interaction with water

The five representative conformers were reoptimized using the ESFF force field in Insight 97. Table 1 compares the optimal energies obtained by using the UFF and ESFF force fields.

The data confirm that the order of relative energies of the conformers remain unchanged when switching from the UFF to the ESFF force field. The energy range involved widened only from about 1 kcal/mol to about 7 kcal/mol.

All five conformers were soaked with a 5.0-Å-thick water layer, and the hydrated assemblies were optimized. Color Plate 2 depicts the effect of hydration on the geometries of the representative conformers.

Evidently, interaction with water has only moderate effects on the geometry. Although some randomly occurring hydrogen bonds were present in the initial geometry, several additional hydrogen bonds are formed during the energy minimization. Table 2 summarizes the initial (n_i) and final (n_f) number of hydrogen bonds as well as the total number (N_{tot}) of water molecules in the soaking layer.

The number and range of initial random hydrogen bonds (0–3) involving the different conformers increased significantly (to 5–12) as the optimal geometry was reached. Generally, the more coiled a conformer is, the less number of hydrogen bonds it is able to form. Color Plate 3 depicts conformer 3 with the 10 water molecules in its primary hydrate layer. The left pane in Color Plate 4 shows conformer 5 with the 5 water molecules in its primary hydrate layer, and the solvent-accessible Connolly surface of the same conformer is presented in the right pane.

As expected, the location of the water molecules in both illustrative structures (conformers 3 and 5) correlates with the position of the oxygen atoms in the hydrophilic chain and with the highly charged regions on the corresponding Connolly surface (Color Plate 4). Color Plate 4 also provides an explanation for why the highly coiled conformations have less water molecules bound than the noncoiled ones. Evidently, in a highly coiled conformation, some of the oxygen atoms and their highly charged sites are sterically hindered from the water molecules and, consequently, hydrogen bonds are less likely to form. Since the probability of highly coiled conformers increases with the length of the OE chain, such steric hindrance should become more pronounced in OPE_n components with $n > 10$.

The number of bound water molecules n_f averaged over the five representative conformers in Table 2 is $<n_f> = 9.4$. This is in agreement with experimental findings obtained in reverse micellar systems of numerous polyoxyethylene surfactants in a variety of nonpolar solvents. Depending on temperature and the nature of the actual amphiphile and solvent, experiments indicate that if sufficient amount of water is present in the solution each OE segment of the chain is hydrated by ~1 water molecule.[26] Upon further increasing the water content of the solution first the formation of an aqueous pool in the polar core of the reverse micelle (where the OE chains of the surfactant are located) is observed. Then, above certain critical value of the water content, phase separation occurs.

CONCLUSIONS

The described atomic level modeling reveals that the energy distribution of the different most probable conformers of the OPE_9 molecule is relatively narrow, and that interaction with water modifies the geometry of the conformers only slightly. The possible overall shape of the molecule ranges between two extreme structures associated with a straight and a tightly packed (coiled) OE chain. Automatic clustering procedure yields 11 clusters, in which the torsional angles show narrow distribution around only a few certain values. No correlation was found between the torsional angles and the energy.

The Connolly surface proved its utility in predicting the locations for potential hydrogen bonds. For the five different representative conformers investigated, 5–12 such bonds were found. The straight-chain conformer has the highest, and the globular one has the lowest, number of hydrogen bonds. The number of hydrogen bonds n_f averaged over the representative conformers ($<n_f> = 9.4$) is in accord with experimental findings. Each water molecule in the primary hydrate layer is found to participate in only one hydrogen bond with the OPE_9.

REFERENCES

1 Schick, M.J. (ed.). *Nonionic Surfactants.* Marcel Dekker, New York, 1987

2 Zana, R. (ed.). *Surfactant Solutions.* Marcel Dekker, New York, 1987

3 Gu, J., and Schelly, Z.A. Comparative phase behavior about the L_2 phase of ternary and quaternary systems of

Triton X-100 and its separated *p-tert*-OPE$_n$ (n = 5, 7, and 9) components in cyclohexane. *Langmuir* 1997, **13**, 4251–4255
4 Zhou, Z., Chu, B., and Nace, V.M. Association behavior a triblock copolymer of oxyethylene (E) and oxybutylene (B). A study of $B_5E_{91}B_5$ in aqueous solution. *Langmuir* 1996, **12**, 5016–5021
5 Shiloach, A., and Blakschtein, D. Measurement and prediction of ionic/nonionic mixed micelle formation and growth. *Langmuir* 1998, **14**, 7166–7182
6 Kostarelos, K., Tadros, T.F., and Luckham, P.F. Physical conjugation of (tri-)block copolymers to liposomes toward the construction of sterically stabilized vesicle systems. *Langmuir* 1999, **15**, 369–376
7 Eicke, H.-F., and Parfitt, G.D. (eds.). *Interfacial Phenomena in Apolar Media*. Marcel Dekker, New York, 1987
8 Palmer, B.J., and Liu, J. Effects of solute–surfactant interactions on micelle formation in surfactant solutions, *Langmuir* 1996, **12**, 6015–6021
9 Palmer, B.J., and Liu, J. Simulations of micelle self-assembly in surfactant solutions. *Langmuir* 1996, **12**, 746–753
10 Shinto, H., Tsuji, S., Miyahara, M., and Higashitani, K. Molecular dynamics simulations of surfactant aggregation on hydrophilic walls in micellar solutions. *Langmuir* 1999, **15**, 578–586
11 Wendoloski, J.J., Kimatian, S.J., Schutt, C.E., and Salemme, F.R. Molecular dynamics simulation of a phospholipid micelle. *Science* 1989, **243**, 636–638
12 Watanabe, K., Ferrario, M., and Klein, M.L. Molecular dynamics study of a sodium octanoate micelle in aqueous solution. *J. Phys. Chem.* 1988, **92**, 819–821
13 Watanabe, K., and Klein, M.L. Molecular dynamics studies of sodium octanoate and water: The liquid-crystal mesophase with two-dimensional hexagonal symmetry. *J. Phys. Chem.* 1991, **95**, 4158–4166
14 Laaksonen, L., and Rosenholm, J.B. Molecular dynamics simulations of the water/octanoate interface in the presence of micelles. *Chem. Phys. Lett.* 1993, **216**, 429–434
15 Shelley, J.C., Sprik, M., and Klein, M.L. Molecular dynamics simulation of an aqueous sodium octanoate micelle using polarizable surfactant molecules. *Langmuir* 1993, **9**, 916–926
16 Bocker, J., Brickmann, J., and Bopp, P. Molecular dynamics simulation study of an *n*-decyltrimethylammonium chloride micelle in water. *J. Phys. Chem.* 1994, **98**, 712–717
17 MacKerell, A.D., Jr. Molecular dynamics simulation analysis of a sodium dodecyl sulfate micelle in aqueous solution: Decreased fluidity of he micelle hydrocarbon interior. *J. Phys. Chem.* 1995, **99**, 1846–1855
18 Bast, T., and Hentschke, R. Molecular dynamics simulation of a micellar system: 2,3,6,7,10,11-Hexakis(1,4,7-trioxaoctyl)triphenylene in water. *J. Phys. Chem.* 1996, **100**, 12162–12171
19 Alaimo, M.H., and Kumosinski, T.F. Investigation of hydrophobic interactions in colloidal and biological systems by molecular dynamics simulations and NMR spectroscopy. *Langmuir* 1997, **13**, 2007–2018
20 Rappé, A.K., Casewit, C.J., Colwell, K.S., Goddard, W.A., III, and Skiff, W.M. UFF, a full periodic table force field for molecular mechanics and dynamics simulations. *J. Am. Chem. Soc.* 1992, **114,** 10024–10035
21 Molecular Simulations. *Forcefield-Based Simulations.* Molecular Simulations, Inc., San Diego, California, April 1997
22 Casewit, C.J., Colwell, K.S., and Rappé, A.K. Application of a universal force field to organic molecules. *J. Am. Chem. Soc.* 1992, **114**, 10035–10046
23 Casewit, C.J., Colwell, K.S., and Rappé, A.K. Application of a universal force field to main group compounds. *J. Am. Chem. Soc.* 1992, **114**, 10046–10053
24 Rappé, A.K., Colwell, K.S., and Casewit, C.J. Application of a universal force field to metal complexes. *Inorg. Chem.* 1993, **32**, 3438–3450
25 Derecskei, B., Derecskei-Kovacs, A., and Schelly, Z.A. Atomic level molecular modeling of AOT reverse micelles. I. The AOT molecule in water and carbon tetrachloride, *Langmuir* 1999, **15,** 1981–1992
26 Doyle, M.H., McDonald, M.P., Rossi, P., and Wood, R.M. Dielectric studies of a nonionic surfactant–alkane–water system at low water content. In: *Microemulsions* (Robb, I.D., ed.). Plenum, New York, 1982, pp. 103-114; and references therein